Research Article

The Influence of Surfactant HLB and Oil/Surfactant Ratio on the Formation and Properties of Self-emulsifying Pellets and Microemulsion Reconstitution

Irini Matsaridou,[1] Panagiotis Barmpalexis,[1] Andrea Salis,[1] and Ioannis Nikolakakis[1,2]

Abstract. Self-emulsifying oil/surfactant mixtures can be incorporated into pellets that have the advantages of the oral administration of both microemulsions and a multiple-unit dosage form. The purpose of this work was to study the effects of surfactant hydrophilic–lipophilic balance (HLB) and oil/surfactant ratio on the formation and properties of self-emulsifying microcrystalline cellulose (MCC) pellets and microemulsion reconstitution. Triglycerides (C_8–C_{10}) was the oil and Cremophor ELP and RH grades and Solutol the surfactants. Pellets were prepared by extrusion/spheronization using microemulsions with fixed oil/surfactant content but with different water proportions to optimize size and shape parameters. Microemulsion reconstitution from pellets suspended in water was evaluated by turbidimetry and light scattering size analysis, and H-bonding interactions of surfactant with MCC from FT-IR spectra. It was found that water requirements for pelletization increased linearly with increasing HLB. Crushing load decreased and deformability increased with increasing oil/surfactant ratio. Incorporation of higher HLB surfactants enhanced H-bonding and resulted in faster and more extensive disintegration of MCC as fibrils. Reconstitution was greater at high oil/surfactant ratios and the droplet size of the reconstituted microemulsions was similar to that in the wetting microemulsions. The less hydrophilic ELP with a double bond in the fatty acid showed weaker H-bonding and greater microemulsion reconstitution. Purified ELP gave greater reconstitution than the unpurified grade. Thus, the work demonstrates that the choice of type and quantity of the surfactant used in the formulation of microemulsions containing pellets has an important influence on their production and performance.

KEY WORDS: disintegration and mechanical properties; FT-IR and H-bonding; microemulsion reconstitution; self-emulsifying pellets; surfactant HLB and oil/surfactant ratio.

INTRODUCTION

Pellets containing self-emulsifying drug delivery systems of oil, surfactant, and drug present advantages in the oral administration of poorly soluble drugs. As a multiple-unit dosage form, they assist smooth passage in the gut and, because of the formation of microemulsion in contact with gastric fluids, they present the drug dissolved in fine oil/surfactant droplets. Therefore, stability and absorption are improved and dose dumping and variability in plasma levels are minimized (1). The self-emulsifying oil/surfactant mixtures, also named self-emulsifying systems (SES) can be incorporated into pellets of microcrystalline cellulose (MCC) as oil in water microemulsions, during the process of wet extrusion-spheronization and these pellets do in fact release the drug *in vivo* in dogs as if they were the microemulsion liquid itself (2).

It has also been found that the relative quantities of SES and water, as well as the fraction of oil and surfactant in the dry pellets affect the amount of liquid and SES that could be incorporated into MCC, the extrusion force, and the proper-

ties of the pellets (1,3,4). Even when included in the pellets just as single components, surfactants influence the pellet quality. Hydrophilicity of surfactant was found to affect its concentration in the wetting liquid and the median pellet size, whereas the added level determined the rheological properties of the extruded water mass and the median pellet size (5,6).

In addition, emulsion stability is known to be affected by the HLB of the surfactant and the oil/surfactant ratio. An HLB range of 10–15 has been suggested for stable emulsions with finer droplet diameter (7). Therefore, the HLB of the surfactant is also expected to affect pellet formation and quality when added as self-emulsifying wetting microemulsion. Furthermore, higher oil content may be desirable in order to dissolve more drug in the self-emulsifying mixture and increase its content in the pellet, but there is a limit imposed on this, due to the possible adverse effect on emulsion stability and droplet size (8,9).

So far, there are no literature data for the single or combined effects of HLB of the surfactants and of the oil/surfactant ratio on the preparation and the properties of pellets, and microemulsion reconstitution from the SES present in the dry pellets. Therefore, the purpose of this study was to prepare MCC pellets containing a fixed amount of SES, using microemulsions as wetting liquids, and to evaluate the single

[1] Department of Pharmaceutical Technology, School of Pharmacy, Aristotle University of Thessaloniki, Thessaloniki, 54 124, Greece.
[2] To whom correspondence should be addressed. (e-mail: yannikos@pharm.auth.gr)

and combined effects of HLB and oil/surfactant ratio on the size distribution and shape of the pellets, on their mechanical properties and disintegration, and on the reconstitution ability of microemulsions, by applying factorial design and statistical analysis.

Medium-chain triglycerides was the oil and four non-ionic surfactants of similar chemical nature but different HLB's were the self-emulsifying components included at three oil/surfactant ratios 1.5, 2.3, and 3.1, but a fixed 20% *w/w* proportion of final dry pellets. Ternary diagrams together with droplet size analysis by dynamic light scattering were used to determine regions of microemulsion formation subsequently used for the preparation of pellets. Reconstitution of microemulsions from the pellets suspended in water was evaluated using turbidimetry. Finally, infra-red spectroscopy and second derivative spectra were applied to elucidate interactions between surfactants and MCC.

MATERIALS AND METHODS

Materials

Microcrystalline cellulose (Avicel® PH-101, lot 6950C, FMC Ireland) was used as the pellet-forming material. The oil phase of the self-emulsifying mixtures consisted of medium-chain triglycerides of caprylic/capric esters; C_8: 59.6%, C_{10}: 39.9%, C_{14}: 0.4%, (Radia 7104, Oleon N.V., Oelegen, Belgium). The surfactants were esters of glycerides with ethoxylated ricinoleic acid (Cremophor EL and purified EL (ELP)), or hydroxystearic acid (Cremophor RH 40), and polyethylene glycol esterified with ethoxylated hydroxystearic acid (Solutol HS 15). All surfactants were generous gifts from BASF AG, Germany. Distilled water was added as the external phase of the microemulsions. The chemical structures of oil and surfactants are shown in Fig. 1.

Molecular Weights and HLB of Surfactants

For Cremophors, molecular weights (MW) were taken from BASF (Technical Information May 2010) and for Solutol HS 15 with defined composition of ethoxylated hydroxystearic acid ester (70%, MW=960) and free ethylene glycol (30%, MW=62), it was calculated from their chemical structures (Fig. 1) and the mass balance of the two components.

Only ranges of HLB values for the experimental surfactants are available in the literature, and since Cremophors are now produced as pure substances and Solutol is a defined mixture, the HLB values were derived directly from the molecular structures of Cremophors ELP, RH 40, and RH 60 (Fig. 1), and in the case of Solutol, from the chemical structures and the mass balance of the two components. According to Griffin's expression,

$$HLB = 20[1 - (mass\ of\ hydrophobic\ part/total\ molecular\ mass)] \tag{1}$$

Therefore, from Fig. 1, considering the carbonyl (–CO–) group and the part to its left as hydrophilic and the part to its right as hydrophobic, HLB values were calculated, where the hydrophobic part and total molecular mass are: for ELP/EL 759 and 2,472, for RH 40 765 and 2,698, and for RH 60 765 and 3,578, respectively. For Solutol, the HLB was calculated from the HLB of the ethoxylated hydroxystearic ester which is $14.7 = 20[1-(255/960)]$, the HLB of free polyethylene glycol, taken as 20 due to its hydrophilic character, and by application of the mass balance according to their proportions in the surfactant. Hence, HLB of Solutol is $(0.7 \times 14.7) + (0.3 \times 20) = 16.3$.

Surface Tension and Critical Micelle Concentration

Surface tension of the surfactant solutions in water (0.1% *w/v*) was measured using a du Nuoy ring interfacial tensiometer (Kruss 8600, Germany). Three repetitions were made and
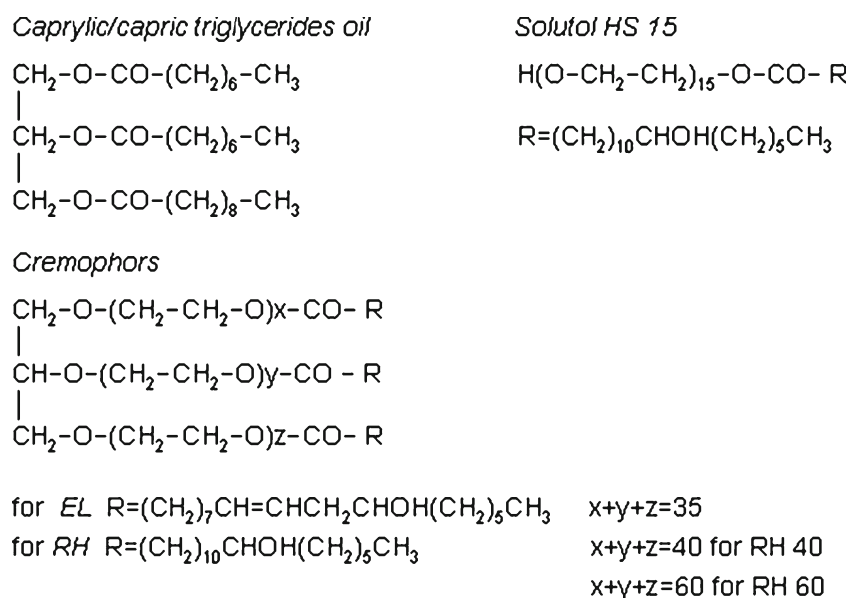
Caprylic/capric triglycerides oil

$$CH_2-O-CO-(CH_2)_6-CH_3$$
$$|$$
$$CH_2-O-CO-(CH_2)_6-CH_3$$
$$|$$
$$CH_2-O-CO-(CH_2)_8-CH_3$$

Cremophors

$$CH_2-O-(CH_2-CH_2-O)x-CO-R$$
$$|$$
$$CH-O-(CH_2-CH_2-O)y-CO-R$$
$$|$$
$$CH_2-O-(CH_2-CH_2-O)z-CO-R$$

for *EL* $R=(CH_2)_7CH=CHCH_2CHOH(CH_2)_5CH_3$ $x+y+z=35$

for *RH* $R=(CH_2)_{10}CHOH(CH_2)_5CH_3$ $x+y+z=40$ for RH 40
    $x+y+z=60$ for RH 60

Solutol HS 15

$$H(O-CH_2-CH_2)_{15}-O-CO-R$$

$$R=(CH_2)_{10}CHOH(CH_2)_5CH_3$$

Fig. 1. Chemical structures of components in self-emulsifying mixtures

the mean value taken. Critical micelle concentrations of surfactants in water were determined by measuring the surface tensions (γ, mN/m) of a series of solutions of different concentrations ($C\%$ w/v), from 0.0001 to 0.1% w/v. From the surface tension vs logarithm concentration plots, the C value corresponding to a sharp surface tension drop to a constant value, or the range of C values corresponding to a gradual decrease to constant concentration, were recorded (10).

Ternary Diagrams

Ternary phase diagrams were constructed by adding water dropwise to different oil/surfactant ratios from 9:1 (90% oil), to 1:9 (10% oil) at a constant rate of about 2 ml/min, under agitation with magnetic stirrer. This process resembles mixing of the oil/surfactant with gastric fluids. The different phases formed (emulsion, clear dispersion, and gel) were observed macroscopically after the addition of every water drop and the regions corresponding to the different phases were drawn in the diagrams by connecting the proportions of surfactant/oil/water at the boundaries of each phase. Microemulsions with droplet diameter between 100 and 300 nm were further identified from droplet size measurements as described below.

Droplet Size

Average hydrodynamic diameter of the microemulsions was estimated by Dynamic Light Scattering using a Zetasizer (ZEN3600, Malvern Instruments Ltd, UK) at 25°C. The diameter is derived from the change of intension pattern of scattered light with time (laser 633 nm, angle detection 173°), which depends directly on the diffusivity of the droplets. For measurements with polydispersity index PDI<0.5, the estimated diameters represent z-cumulants obtained directly from the instrument, whereas for measurements with PDI>0.5 due to the broadness or to the presence of more than two peaks, the diameters represent the median of the light intensity-diameter distributions.

Preparation of Wetting Microemulsions and Pellets

Amounts of 7.5 g of SES mixtures were initially prepared by mixing oil with surfactant at three oil/surfactant ratios 1.5 (or 6:4), 2.3 (or 7:3), and 3.1 (or 7.55:2.45), by increasing at a fixed step of 0.8. As it was found from droplet size measurements presented later in the paper, these ratios gave generally more stable microemulsions, with average droplet diameter less affected by dilution with water (11). The oil/surfactant mixtures were next heated to 60°C to form clear solutions and 22.5 g of deionized water was added to give 30 g microemulsions, consisting of 75% water and 25% w/w oil/surfactant (×4 water dilution), which was the starting wetting liquid.

For the preparation of pellets, 30 g of MCC powder was mixed in a cylindrical mixing vessel fitted with a paddle stirrer for about 5 min with 30 g of the prepared microemulsion. Depending on the surfactant and oil/surfactant ratio, further addition of 2 to 7 g water, resulting in total of 76.5 to 79.7% w/w of wetting liquid, was required to obtain a wet mass most suitable for the production of spherical pellets with narrowest size distribution (different formulations were obtained by increasing water level by 1 ml each time, until the shape of the pellets became most spherical). A radial extruder (Model 20, Caleva, UK) fitted with a 1-mm circular orifice screen and a spheronizer (Model 120, Caleva, UK), fitted with a cross-hatch friction plate, rotating at 4,500 for 10 min were used. The pellets were dried at 50°C for 5–6 h, in an air-circulation tray oven (UT6, Heraeus Instruments, Germany).

Physical Properties and Moisture Content of Pellets

Moisture content was measured by heating about 3 g accurately weighed samples at 105°C, on a Halogen Moisture Analyzer (HR73 Mettler Toledo). The weight was monitored every 30 s and measurement was stopped when the weight loss between two successive measurements was <0.01 g. The pycnometric density of the pellets was measured with a helium pycnometer (Ultrapycnometer 1000, Quantachrome Instruments, USA) and the bulk and tapped densities with a J. Engelsmann volumeter (drop height 1.5 mm, Model JEL ST 2, Germany).

Size distribution and mean diameter were determined by placing approximately 10 g of pellets on a stack of small 10 cm diameter sieves (DIN/ISO3310-1, Retch, Germany), of 300, 425, 600, 850, and 1,200 µm aperture, and vibrating for 10 min (Fritsch Analysette 3, Oberstein, Germany). Median pellet diameter was derived from cumulative weight plots from the data of sieve aperture and weight of remaining pellets. Shape of the pellets was determined from two-dimensional images after examination of more than 100 pellets of the modal fraction 850–1,200 µm in three to four fields at a total magnification 6.5×5=32.5 using image processing and analysis system comprised of stereomicroscope fitted with top cold light source (Olympus SZX9, Japan and Highlight 3100, Olympus Optical), video camera (VC-2512, Sanyo Electric, Japan), and software (Quantimet 500, Cambridge, England). It was expressed as the shape factor e_R (12) which is sensitive to small shape variations and has a value of one for perfect spheres.

Mechanical Properties

Pellets of 1,000–1,180 µm in diameter were characterized by recording their diametric loading–deformation curve in a modified CT-5 machine (Engineering System, Nottingham, UK), at a testing speed of 1 mm/min, until crushing (13). A 25-N subminiature load cell (model ELFM-T2M, Entran, USA) connected to a signal amplifier (RDP E308) was used, and the signals were collected with a polymeter (Handyscope, Holland) and recorded in a computer as Excel files. Deformability was expressed as the inverse of the slope of the force–displacement curve, and particularly the part starting from the initial point of force increase to the first peak recorded, corresponding to the crushing load.

Disintegration

The disintegration time of pellets 1,000–1,200 µm in diameter was determined in a modified reciprocating cylinder USP Apparatus 3 (Bio-Dis RRT9, G.B. Caleva,

UK). The cylinders were fitted at the bottom with 840-μm nylon grids and were immersed in wider thermostatted glass vessels (1-l beakers) filled with deionized water, in order to avoid exit and turbulence. Standard tablet disintegration disks of increased diameter equal to the internal cylinder diameter were used so as to enable smooth sliding inside the cylinder during testing (disk moving in the opposite direction to the cylinder movement) and apply light pressure to the pellets against the grid upon reaching the bottom of the cylinder after a dip. Thirty milligrams of pellets were tested at a temperature of 37±0.5°C, and cylinder dip rate of 20 dpm, until no pellets were left in the cylinder. The results represent means of three determinations.

FT-IR Spectroscopy

Spectra were obtained using a Shimadzu FT-IR-Prestige-21 spectrometer (Shimadzu Co. Japan) attached to a horizontal Golden Gate MKII single-reflection ATR system (Specac, Kent, UK) equipped with a Diamond/ZnSe crystal (45° angle to IR beam, 1.66 microns at $1,000\ cm^{-1}$ depth of penetration, 2.4 refractive index, and $525\ cm^{-1}$ long wavelength cut-off). A small amount of pellets with the same oil/surfactant ratio 2.3 was placed on the diamond disk and scanned for absorbance from 4,000 to $500\ cm^{-1}$ at resolution $4\ cm^{-1}$. Second derivative spectra were obtained according to the Savitzky–Golay method after smoothing, using the IR Solution software program (Shimadzu Co. Japan).

Reconstitution of Microemulsions from Pellets

The ability of the oil/surfactant mixture present in the pellets to re-emulsify was evaluated using a USPII rotating paddle dissolution apparatus (Pharma-Test, Germany). A 2.5-g sample of pellets corresponding to 0.5 g self-emulsifying mixture were placed in 200 ml distilled water of 37°C and agitated at 100 rpm. This oil/surfactant dilution ensured that during the testing time of 3 h, reconstitution reached completion for most pellet formulations with light transmittance approaching a constant value within the reading range of the instrument.

Five-milliliter samples were withdrawn at time intervals of 2, 15, 30, 60, 120, and 180 min, placed in screw-capped glass test tubes and analyzed for transmittance ($T\%$; λ=850 nm) using a
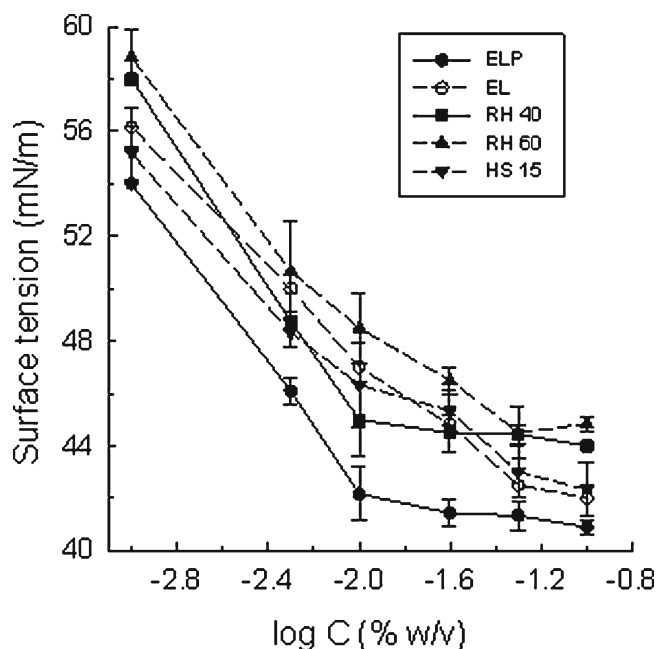
Fig. 2. Surface tension as a function of surfactant concentration in aqueous solutions for determination of critical micelle concentration

turbidimeter (TURBISCAN Classic, MA2000, Formulaction, France), calibrated for T=100% with special silicon oil.

Transmittance was measured directly or after centrifugation of the samples for 3 min at 4,000 rpm in a laboratory centrifuge (Labofuge 400R, Heraeus, Germany), which ensured removal of any disintegrating MCC, so that total transmittance from that due to re-emulsification could be distinguished.

Statistical Analysis

For the statistical analysis the SPSS 11.5 statistical software was used (SPSS Inc Chicago, IL, USA).

RESULTS AND DISCUSSION

Self-emulsifying microemulsions offer the possibility of solubilization of poorly water soluble drugs and their

Table I. Properties of the Self-emulsifying Materials

Material	MW[a]	HLB	Density[b] (g/cc)	Melting point[b] (°C)	Surface tension (mN/m)[c]	CMC (% w/v)
Surfactant						
Cremophor ELP	2,500	13.9	1.06	20	41.3 (0.30)[d]	0.01
Cremophor EL	2,500	13.9	1.06	20	42.0 (0.01)	0.01–0.05
Cremophor RH40	2,500	14.3	1.04	30	44.0 (0.01)	0.01
Cremophor RH60	2,800	15.7	1.04	27	44.8 (0.3)	0.005–0.05
Solutol HS15	691	16.3	1.05	30	42.3 (0.40)	0.01–0.05
Oil						
Radia7104	498	–	0.95	−11	–	–
(Medium-chain triglycerides)						

[a] For ELP, EL, RH 40, and RH 60 molecular weight data from BASF and for Solutol calculated from the chemical structure
[b] Data from BASF and Handbook of Pharmaceutical Excipients
[c] 0.1% w/v aqueous solution
[d] SD, n=3

presentation in the gut dissolved in fine droplets, thus avoiding the dissolution step of dispersed powder that limits absorption (14). Also, the lipids can increase gastric retention time and for highly lipophilic drugs, may also enhance lymphatic transport and bioavailability by reducing first-pass metabolism (15). Medium-chain triglycerides are preferred due to their rapid digestion, and non-ionic surfactants because they are less toxic than the ionic, less affected by pH and ionic strength and improve dissolution and absorption of drugs (16–19). Furthermore, incorporation of SES with dissolved drug into pellets provides a presentation with the advantages of a multi-unit form (1).

Physicochemical Properties of Surfactants

In Table I data for MW and HLB of surfactants calculated from their chemical structures (Fig. 1) as described in "MATERIALS AND METHODS" are presented. In addition, densities and melting points obtained from the literature and measured values of surface tension of 0.1% w/v aqueous solutions of surfactants, together with critical micelle concentrations are also presented. From the results in Table I it can be seen that all Cremophors have similar MW's but different values of HLB ranging from 13.9 to 15.7. Solutol has about four times lower MW than that of Cremophors but higher HLB value of 16.3. Although the range of HLB of the chosen surfactants is not very broad, this is compensated by their very similar chemical nature so that the effects of hydrophilicity can be unambiguously estimated. In addition, all surfactants have similar densities (1.04–1.06 g/cc). The melting point of ELP and EL is 20°C being viscous liquids at room temperature and RH 40, RH 60, and Solutol have melting points between 20 and 30°C, indicating a semisolid nature. All surfactants reduced the surface tension of distilled
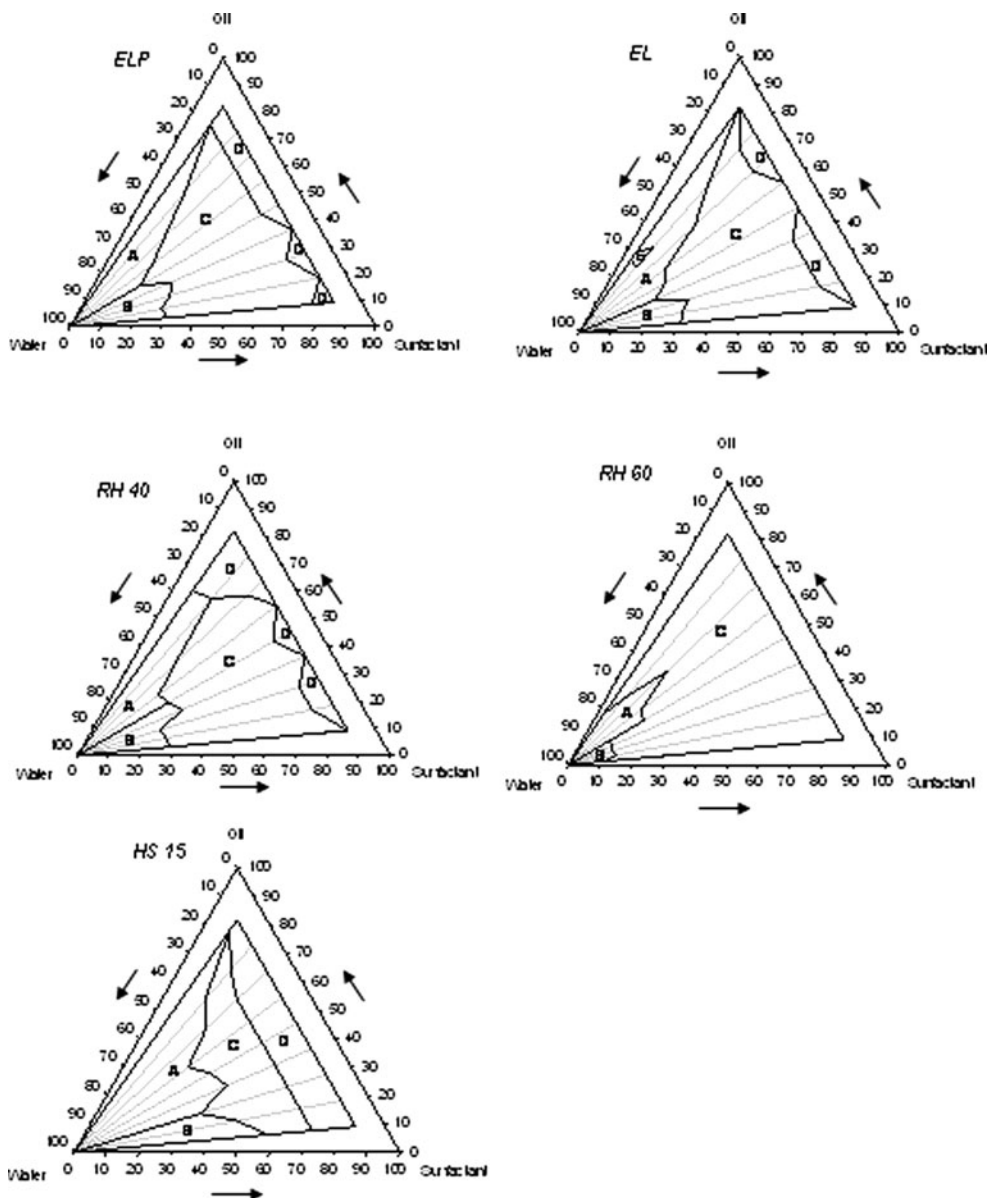

Fig. 3. Ternary phase diagrams of water–surfactant–oil mixtures showing areas of formation of emulsion (**a**), clear dispersion (**b**), gel (**c**), turbid dispersion (**d**), and frothy viscous dispersion (**e**)

water from a measured value of 72.1 to between approximately 41 and 45 mN/m.

Furthermore, it is noticed that Cremophors ELP and RH 40 have a specific CMC of 0.01% *w/v*, corresponding to a sharp drop of surface tension in the surface tension–concentration plot shown in Fig. 2, indicating that they are pure surfactants. On the contrary, Cremophors EL and RH 60 have a CMC range, corresponding to the gradual drop of surface tension, which begins at 0.01 and reaches a constant value at 0.05% *w/v*, indicating the presence of free fatty acids or esters other than the esters of glyceride with ethoxylated ricinoleic acid for EL and ethoxylated hydroxystearic acid for RH 60, of different micelle structure (BASF, Technical Information, July 2008, and reference (20). Solutol also shows a gradual drop of surface tension over a CMC range of 0.01–0.05% *w/v*, which however is expected as it is a mixture of ester of polyethylene glycol with ethoxylated hydroxystearic acid and free polyethylene glycol (BASF, Technical Information, July 2009).

Ternary Diagrams and Droplet Size Analysis

In Fig. 3, ternary phase diagrams of water/surfactant/oil mixtures are presented. By moving along the lines in the diagram from 0 to 100% water (left-hand lower apex), it is noticed that except in the case of RH 60, addition of water to mixtures of oil/surfactant ratios from 1:9 (10% oil) to 9:1 (90% oil) generally results in the formation initially of turbid dispersion (zone D) followed by a viscous gel (zone C). For RH 60 gel is formed directly. In all cases, further water addition results in a milky emulsion (zone A) when oil/surfactant is from 4:5 or 5:5 to 8:2 or 9:1 for the Cremophors and from 3:7 to 8:2 for Solutol. For lower oil/surfactant ratios, further addition of water to the gel results in a transparent bluish dispersion (zone B) formed by surfactant micelles (21). An additional zone (E) is seen in the diagram of EL near oil/surfactant ratio 9:1 and water content 60–70%, representing frothy and viscous texture, possibly due to the presence of traces of substances other than the main component (previously discussed for Fig. 2).

From Fig. 3 it can be seen that RH 60 with high HLB value of 15.7 forms emulsion only at high water proportions whereas Solutol which also has an even higher of HLB=16.3, forms emulsions at both low and high water proportions over a much larger area of combinations than the Cremophors. The higher emulsification ability of Solutol should be due to its lower MW (Table I) and hence smaller molecular volume, and also to the fact that it consists of a mixture of surfactants, which contribute to more effective packing in the oil/water interfacial layer and greater interfacial film rigidity (10).

In Table II, results of droplet size analysis by Dynamic Light Scattering (average droplet diameter and standard deviation) are presented for four oil/surfactant ratios 1.5 (or 6:4), 2.3 (or 7:3), 3.1 (or 7.6:2.4), and 3.9 (or 7.9:2.1), increasing progressively by a constant factor 0.8. These ratios were

Table II. Average Droplet Diameter of Microemulsions (SD, *n*=3) of Different Oil/Surfactant Ratios and Water Dilutions and Variability of Diameter Due to Dilution

	Droplet diameter (nm)				
Ratio of oil/surfactant	×4	×40	×400	×4,000	Variability due to dilution (V%)
Cremophor ELP					
1.5	201 (12)	209 (15)	181 (25)	252 (31)	5
2.3	341 (4)	234 (11)	215 (28)	257 (78)	21
3.1	310 (16)	337 (52)	290 (56)	299 (87)	7
3.9	287 (10)	217 (45)	182 (63)	337 (79)	27
Cremophor EL					
1.5	198 (6)	208 (11)	195 (27)	200 (26)	4
2.3	321 (8)	233 (5)	236 (19)	261 (72)	6
3.1	301 (10)	322 (42)	267 (52)	305 (80)	11
3.9	279 (15)	234 (39)	351 (58)	438 (77)	38
Cremophor RH 40					
1.5	211 (7)	231 (6)	166 (24)	205 (46)	13
2.3	319 (6)	260 (3)	211 (24)	231 (52)	18
3.1	227 (8)	232 (15)	221 (19)	222 (7)	2
3.9	242 (7)	197 (11)	313 (17)	420 (25)	33
Cremophor RH 60					
1.5	613 (24)	259 (7)	244 (16)	271 (84)	51
2.3	397 (8)	336 (35)[a]	396 (109)[a]	451 (175)[a]	12
3.1	533 (24)	302 (21)	257 (9)	343 (18)	12
3.9	375 (21)	296 (9)	386 (8)[a]	291 (58)[a]	11
Solutol HS 15					
1.5	115 (1)	100 (2)	79 (1)	77 (1)	19
2.3	191 (1)	103 (1)	129 (5)	97 (1)	33
3.1	227 (16)	196 (26)	221 (44)	426 (110)	40
3.9	225 (4)	514 (183)	466 (216)[a]	1,474 (639)	72

[a] Bimodal distributions: for RH 60/ratio 2.3/dilution ×40 peaks at 631, 148 nm; for ×400 at 194, 817 nm; and for ×4,000 at 543, 64 nm; for RH 60/ratio 3.9/dilution ×400 peaks at 374, 105 nm; for HS 15/ratio 3.9/dilution ×400 at 91, 857 nm

Table III. Wetting Microemulsions (Fixed 7.5 g Oil/Surfactant + Water) Added to 30 g Microcrystalline Cellulose for the Preparation of Pellets, Their Physical Properties, and Moisture Content After Drying

Surfactant/oil/surfactant	Microemulsion		Modal[a] size (%)	Median diameter (μm)	Mean shape factor (e_R)	Density[b] (g/cc)			Moisture content (% dry)
	Total (g)	Water (%)				ρ_s	ρ_b	ρ_t	
ELP/1.5	32	76.5	79	1,074	0.612	1.42	0.68	0.71	1.37
ELP/2.3	32	76.5	81	1,100	0.541	1.44	0.68	0.71	1.62
ELP/3.1	33	77.3	86	1,070	0.521	1.42	0.63	0.67	1.65
RH 40/1.5	33	77.3	75	1,122	0.488	1.44	0.68	0.72	1.51
RH 40/2.3	33	77.3	83	1,120	0.493	1.44	0.63	0.68	1.63
RH 40/3.1	34	77.9	86	1,080	0.510	1.43	0.62	0.67	1.71
RH 60/1.5	34	77.9	84	980	0.523	1.42	0.68	0.71	1.63
RH 60/2.3	35	78.6	89	961	0.565	1.42	0.65	0.66	1.62
RH 60/3.1	35	78.6	86	985	0.664	1.42	0.65	0.68	1.71
HS 15/1.5	35	78.6	92	956	0.532	1.44	0.69	0.71	1.21
HS 15/2.3	36	79.2	92	943	0.591	1.43	0.67	0.70	1.73
HS 15/3.1	37	79.7	84	950	0.380	1.41	0.67	0.69	1.95
EL/2.3	32	76.5	88	1,023	0.530	1.44	0.70	0.71	1.63

[a] 850–1,200 μm
[b] ρ_s, helium density<0.005; ρ_b, bulk density<0.005; ρ_t, tap density<0.02
[c] SD, for shape factor<0.04; ρ_s<0.005; ρ_b<0.03; ρ_s<0.04; ρ_t<0.02

chosen to study, because, as it can be seen from the ternary diagrams in Fig. 3, they cover the region of emulsification in all cases. Size measurements were taken at four water dilutions of oil/surfactant, ×4 (corresponding to wetting microemulsion), ×40, ×400, and ×4,000, to test the variability V (%) of droplet size due to dilution.

$$V(\%) = 100 * \text{SD } \textit{of diameter measured at four dilutions divided by their mean}$$

and represents emulsion stability in presence of increasing water content.

Values of $V(\%)$ are given in Table II where it can be seen that except for emulsions of Cremophor RH 60 at oil/surfactant ratio 1.5 and dilution ×4 and Solutol at ratio 3.9 and dilution ×4,000, the mean diameter is below 466 nm. Furthermore, except for Cremophor RH 60 where the $V\%$ is high (51%) at the lowest ratio 1.5, in all other cases the $V\%$ is highest at oil/surfactant ratio 3.9. This is because of the high diameter measured at dilution ×4,000, which can be ascribed to droplet coalescence due to insufficient surfactant for interfacial film formation and droplet stabilization. The high diameter of emulsion RH 60/ratio 1.5/dilution ×4, causing high variability at ratio 1.5 should be due to its thick texture or high viscosity that may restrict droplet mobility, lowers diffusion coefficient, and increases hydrodynamic diameter.

Preparation and Physical Properties of Pellets

Since oil/surfactant ratios 1.5, 2.3, and 3.1 give microemulsions resistant to dilution, they were used as wetting liquids for the preparation of 12 experimental pellet batches, corresponding to equal number combinations of the two variables under investigation: surfactant type (four levels) and oil/surfactant ratio (three levels). This makes a full factorial design allowing estimation of the main and combined effects (interactions). In addition, a pellet batch with unpurified Cremophor grade EL at
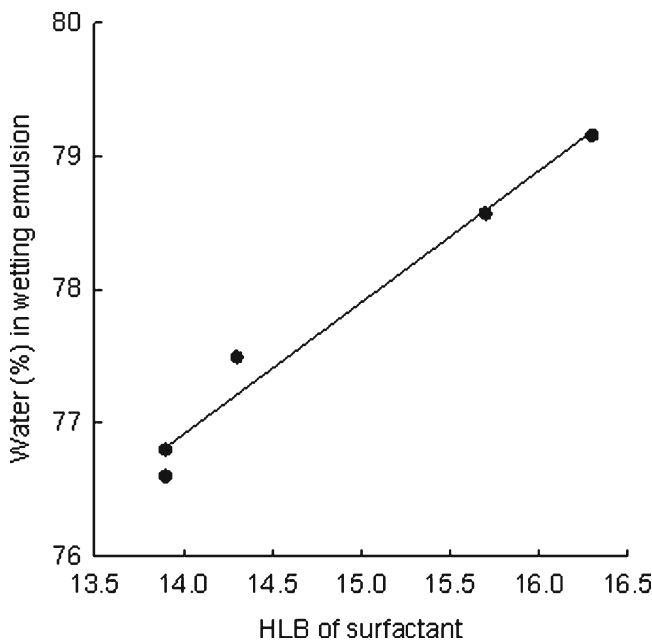

Fig. 4. Percentage of water in the wetting emulsion (%) required for pelletization as a function of the HLB value of the surfactant

Table IV. Mechanical Properties (mean, SD, *n*=8) and Disintegration to Time (Mean, SD, *n*=3) of Pellets

Surfactant/oil/surfactant ratio	Crushing load (N)	Time to break (s)	Deformability (mm/kN)	Disintegration time (min)
ELP/1.5	2.1 (0.2)	4.9 (0.9)	40.5 (9.0)	15.9 (1.1)
ELP/2.3	1.8 (0.1)	4.7 (0.5)	43.3 (5.5)	11.6 (1.2)
ELP/3.1	1.5 (0.2)	4.4 (0.4)	50.0 (9.4)	8.8 (0.4)
RH 40/1.5	2.3 (0.2)	4.6 (0.8)	32.7 (6.7)	9.9 (0.7)
RH 40/2.3	1.6 (0.1)	4.3 (0.4)	46.1 (7.8)	8.4 (0.5)
RH 40/3.1	1.3 (0.1)	4.6 (0.6)	58.3 (9.9)	8.0 (0.6)
RH 60/1.5	2.1 (0.2)	4.0 (0.5)	32.2 (7.1)	10.9 (1.0)
RH 60/2.3	1.6 (0.2)	4.1 (0.6)	44.1 (6.6)	8.6 (0.6)
RH 60/3.1	1.2 (0.2)	4.2 (0.5)	58.0 (9.9)	8.2 (0.8)
HS 15/1.5	2.0 (0.2)	5.4 (0.9)	45.0 (9.5)	7.3 (0.3)
HS 15/2.3	1.7 (0.1)	5.0 (1.1)	50.6 (9.8)	7.9 (1.4)
HS 15/3.1	1.4 (0.1)	4.3 (0.8)	60.1 (8.6)	7.8 (1.0)
EL/2.3	1.8 (0.3)	4.2 (0.2)	38.4 (8.8)	11.8 (1.1)

ratio 2.3 was prepared to compare with the pellets of purified grade (ELP). Only one ratio of EL was compared because its chemical structure and hence HLB is basically the same with that of ELP and therefore experiments with further ratios would contribute little information. A starting combination of 7.5 g oil/surfactant (25% *w/w*) and 22.5 g deionized water (75% *w/w*) was chosen because as seen in Fig. 3 (zone A), at this water proportion, emulsions with Cremophors are formed over a greater range of oil/surfactant ratios and also to avoid production of soft pellets that may form at low water levels which could mask the effect of ratio on deformability (3).

In Table III, the total amount of microemulsion added and the water content (%) in the microemulsion, for the fixed oil/surfactant amount 7.5 g, required to form pellets with narrowest size distribution and most spherical shape are given. In addition, values of median pellet diameter, shape factor e_R, density, and moisture content after drying are also given. In all cases, the total volume increases slightly with oil/surfactant ratio. By comparing the added microemulsion amounts for the different surfactants, it can be seen that on average, they increase in the order ELP/EL<RH 40<RH 60<HS 15 which is the same as the order of increasing HLB value (Table I). Since the amount of oil/surfactant in the microemulsion is fixed, the differences in the added volumes of microemulsion arise from their different water content. This is clearer from Fig. 4 where the average water content (%) is plotted against HLB. It can be seen that water content increases linearly with HLB, which is explained due to the increasing hydration capacity and higher water retention by the more hydrophilic surfactants.

From the result in Table III it can also be seen that all batches have a high percentage (>75%) of pellets in the modal size class 850–1,200 μm, indicating a narrow size range of produced pellets. Pellets are quite spherical in shape as indicated by a mean shape factor e_R above 0.488, except in the case of Solutol ratio 3.1 where the value is low 0.380 due to the inferior quality of the emulsion (Table I) resulting in poor extrusion and rough consistency of extrudate. It is also seen that for Cremophor ELP the shape factor e_R decreases, or the pellets become less spherical and smooth as the surfactant content increases, whereas the opposite is true for the other surfactants (except HS 15/3.1). This should be related to the more hydrophobic character of ELP which may decrease the efficiency of distribution and fixation of the oil/surfactant mixture by the MCC (Table I).

As a result of size and shape uniformity the bulk (ρ_b) and tap (ρ_t) densities are high and within narrow ranges from 0.68 to 0.70 and from 0.67 to 0.72, respectively. Considering the moisture contents of the spheronized and dried pellets, they appear to increase slightly with increasing oil/surfactant ratio but overall they are low,

Table V. Statistical Analysis of the Effects of the Type of Surfactant (A), and Oil/Surfactant Ratio (B), on the Mechanical Properties and Disintegration of Pellets and on the Reconstitution of Microemulsions

	Factor					
	Type of surfactant		Oil/surfactant ratio		$A \times B$	
Measured variable	*p*	η^2	*p*	η^2	*p*	η^2
Mechanical properties and disintegration						
Crushing load	0.106	0.09	0.001	0.72	0.106	0.15
Deformability	0.090	0.10	0.001	0.39	0.470	0.08
Disintegration	0.001	0.83	0.001	0.70	0.008	0.73
Reconstitution after 180 min						
Transmittance (before centrifugation)	0.001	0.84	0.001	0.98	0.001	0.95
Transmittance (after centrifugation)	0.001	0.97	0.001	0.98	0.001	0.94

p statistical significance, η^2 quantitative estimate of the relative importance of the effect with values between 0 and 1

between 1.35 and 1.95 indicating that the water present in the wetting microemulsion and in the wet pellets is easily removed by simple air-circulation tray drying.

Mechanical Properties and Disintegration of Pellets

In Table IV results of the mechanical properties and the disintegration time for the 12 experimental batches of the factorial design are presented. The statistical analysis (ANOVA) for the effects of the two investigated variables on pellet crushing load, resistance to deformation, and disintegration time is presented in Table V. From Table IV it can be seen that in all cases the crushing load decreases whereas deformability increases with increasing oil/surfactant ratio, implying weakening of interparticle bonds and softening due to the presence of oil. This is confirmed in the statistical analysis (Table V) where the effect of ratio is seen to be significant for both crushing load and deformability ($p=$ 0.001, $\eta^2=0.72$ and $p=0.001$, $\eta^2=0.39$), whereas the type of surfactant does not appear to have a significant effect.

Considering the chemical structures of the self-emulsifying components in Fig. 1, it is noticed that all surfactants have fatty acids with –OH groups (position 12) available for H-bonding with MCC, whereas no such groups are present in the triglycerides (oil), resulting in decreased interparticle bonding and hence lower crushing load and higher deformability at higher oil/surfactant ratios.

From the results in Table IV it also appears that the disintegration time decreases with increasing oil/surfactant ratio, but only for the Cremophors, implying significant interaction of the effects of surfactant type and oil/surfactant ratio (Table V, $p=0.008$, $\eta^2=0.73$). This is explicitly shown in the interaction plot in Fig. 5, from which it can be further seen that ELP has longer disintegration time than the others, and that the differences are more pronounced at the lower (1.5) and mid (2.3) ratios. Since surfactants with higher HLB values are expected to impart greater hydrophilicity to the pellets and form stronger H-bonds with MCC, the decrease of disintegration time with increasing HLB should be due to
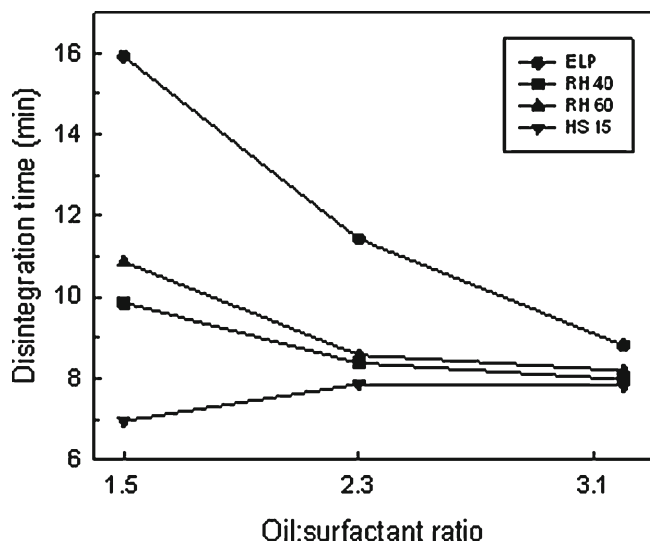
the easier and deeper penetration of water in the pellet. However, the longer disintegration time for the lower oil/surfactant ratio seen for the Cremophors, can be ascribed to the gel formation over larger water proportions (Fig. 3, zone C), hindering movement of water inside the pellet.

FT-IR Spectra

In Fig. 6a, directly obtained FT-IR spectra for MCC powder, the four surfactants (plus spectrum of unpurified EL grade) and the oil are presented. For MCC (a), transmission bands appear in the regions of 3,600–3,200 cm^{-1} assigned to v(OH) stretching modes due to inter- and intra-chain H-bonding, at 3,030–2,780 cm^{-1}, assigned to CH and CH$_2$ stretching modes and unassigned peaks in the fingerprint region below 1,500 cm^{-1} (22,23).

For the surfactants (b–e), shallow bands appear between 3,600 and 3,200 cm^{-1} due to H-bonding, shallow peaks

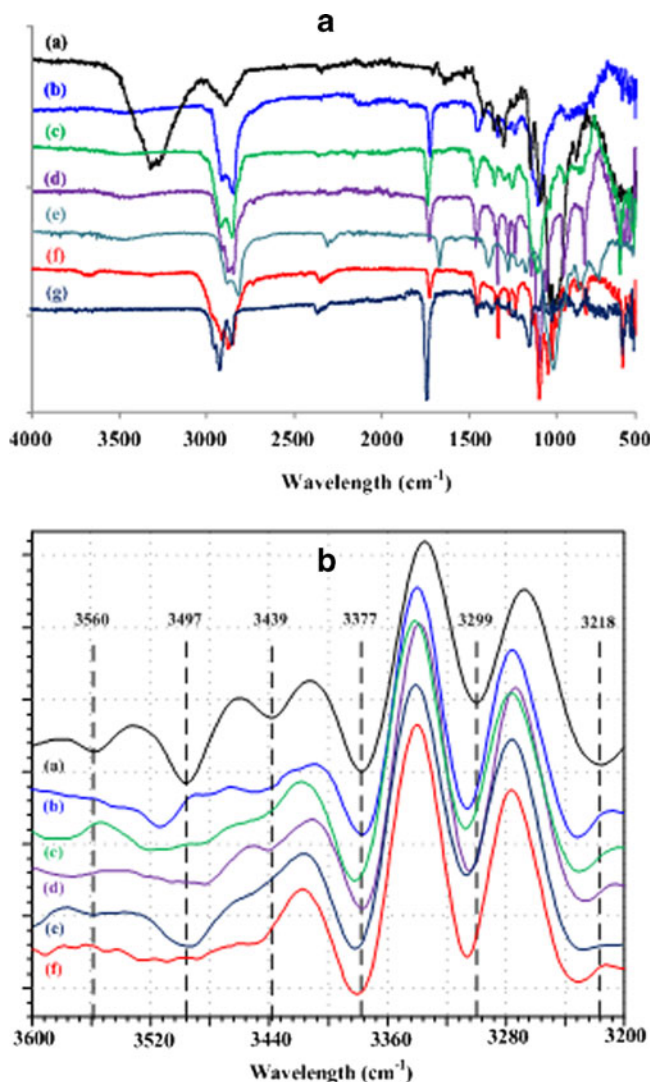**Fig. 5.** Interaction plots of the effects of surfactant type and oil/surfactant ratio on the disintegration time of pellets

Fig. 6. a FT-IR spectra of Avicel (*a*), ELP (*b*), EL (*c*), RH 40 (*d*), RH 60 (*e*), Solutol HS 15 (*f*), and oil (*g*). **b** Second derivative spectra for pellets of MCC only (*a*) and for pellets with self-emulsifying mixtures of ELP (*b*), EL (*c*), RH 40 (*d*) RH 60 (*e*), and Solutol HS 15 (*f*) at fixed oil/surfactant ratio 2.3
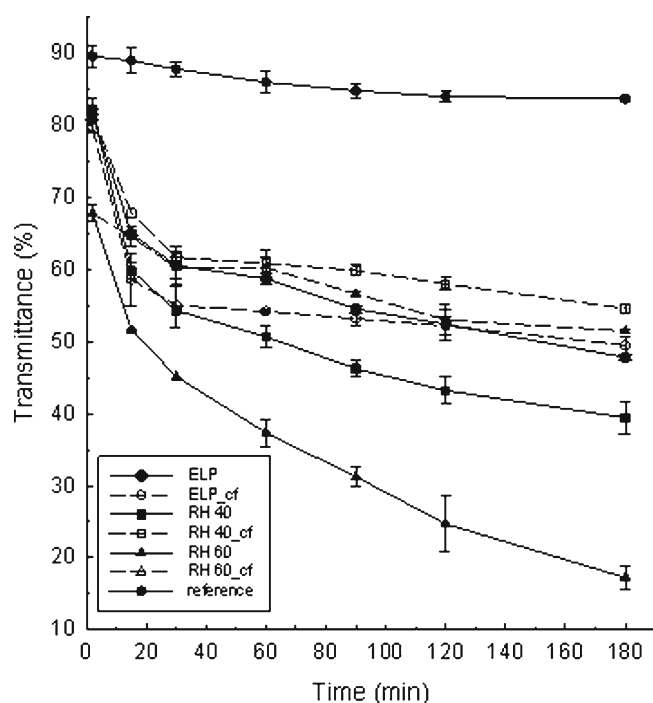
Fig. 7. Plots of transmittance of reconstitution medium before (*solid symbols*) and after centrifugation (*open symbols*, subscript $_{cf}$) with time for pellets with self-emulsifying mixtures of different Cremophor grades at fixed oil/surfactant ratio 2.3

between 3,200 and 2,660 cm^{-1} due to =C–H and C–H stretching modes, between 1,765 and 1,693 cm^{-1} due to C=O stretching vibration modes and unassigned peaks below 1,500 cm^{-1}. For the oil (g), peaks appear between 1,765 and 1,693 cm^{-1} and unassigned peaks below 1,500 cm^{-1}, but there are no peaks in the H-bonding region 3,600–3,200 cm^{-1}. Since between 3,200 and 800 cm^{-1} there is overlapping of the MCC and surfactant peaks, interactions were examined in the region 3,600–3,200 cm^{-1} where MCC shows distinct peaks and the surfactants small bands due to H-bonding. Second

derivative spectra were used for the comparisons, because in these the peaks have greater intensity and hence their position and strength are better distinguished.

In Fig. 6b, the second derivative spectra between 3,600 and 3,200 cm^{-1} are presented for pellets containing MCC only (a) and for pellets containing self-emulsifying mixtures of Cremophors ELP (b), EL (c), RH 40 (d), RH 60 (e), and Solutol (f). Several peaks can be identified in the spectra of MCC pellets and differences from those of self-emulsifying pellets due to interaction of the MCC with the surfactants, appear near 3,560 cm^{-1} and 3,497 cm^{-1}, attributed to intra-chain H-bonds and near 3,439 cm^{-1}, attributed to inter-chain H-bonds in cellulose (24). In particular, the peak near 3,560 cm^{-1} disappears in the self-emulsifying pellets. The peak at 3,497 cm^{-1} is still present in the spectra of ELP, EL, RH 40, and RH 60, although smaller, shifted to the left (higher wavelength) for ELP and EL, and to the right (lower wavelength) for RH 40 and RH 60. The higher wavelength position of the peaks for ELP and EL pellets compared to those for RH 40 and RH 60, indicates a weaker H-bond with MCC. For ELP, EL, and RH 40 the peak at 3,439 cm^{-1} is in the same position indicating weak interactions with MCC, whereas for RH 60 it disappears, indicating stronger interaction.

It is also noticed that in the spectrum of unpurified-grade EL (c) the peaks near 3,497 and 3,439 cm^{-1}, are broader in comparison with those in the spectrum of ELP (b), implying stronger EL-MCC interaction. Since both ELP and EL consist of the same main component (ester of glyceride with ethoxylated ricinoleic acid) the stronger EL-MCC interaction should be due to the presence of minor amounts of free fatty acids or esters in EL other than the main component (discussed for Fig. 2). In the spectra of Solutol pellets (f) both peaks near 3,497 and 3,439 cm^{-1}, disappear implying stronger interaction with MCC, than the other surfactants which is expected due to its highest hydrophilicity (HLB=16.3). Therefore, according to the above discussion, the strength of H-bonding interaction with MCC in increasing order is: ELP<RH 40<RH 60<HS 15 which follows that of increasing HLB.

Table VI. Mean Particle Diameter, Transmittance of the Reconstitution Medium Before (d and T) and after (d_{cf} and T_{cf}) Centrifugation and Total Dispersed Content in the Reconstitution Medium After 180 min (Mean, SD)

Surfactant/oil/surfactant	Mean diameter (nm)		Transmittance (%)		Total dispersed (mg)
	d	d_{cf}	T	T_{cf}	
ELP/1.5	322 (158)	288 (51)	38.0 (2.1)	54.2 (0.4)	170 (9)
ELP/2.3	352 (49)	301 (29)	34.9 (0.7)	44.6 (0.9)	171 (5)
ELP/3.1	345 (217)	237 (45)	33.0 (0.8)	44.8 (0.4)	173 (1)
RH 40/1.5	298 (25)	277 (7)	60.1 (0.7)	72.4 (0.5)	169 (2)
RH 40/2.3	460 (35)	387 (244)	25.5 (3.0)	52.5 (0.5)	212 (8)
RH 40/3.1	398 (56)	324 (57)	23.4 (3.3)	53.0 (0.1)	222 (12)
RH 60/1.5	294 (40)	313 (24)	46.9 (2.8)	66.6 (2.3)	202 (5)
RH 60/2.3	442 (37)[a]	284 (47)	21.6 (2.5)	53.0 (0.1)	244 (6)
RH 60/3.1	398 (56)[b]	324 (57)	14.5 (0.7)	44.3 (0.1)	275 (5)
HS 15/1.5	294 (40)	313 (24)	40.0 (1.3)	54.1 (0.9)	190 (1)
HS 15/2.3	275 (37)	273 (47)[c]	32.0 (2.1)	49.7 (0.8)	207 (3)
HS 15/3.1	389 (172)	330 (101)	31.6 (1.6)	47.8 (0.1)	233 (7)
EL/2.3	349 (37)	295 (27)	35.5 (0.9)	48.4 (1.0)	170 (3)

[a] Bimodal distributions at 603 and 144 nm
[b] Bimodal distributions at 370 and 89 nm
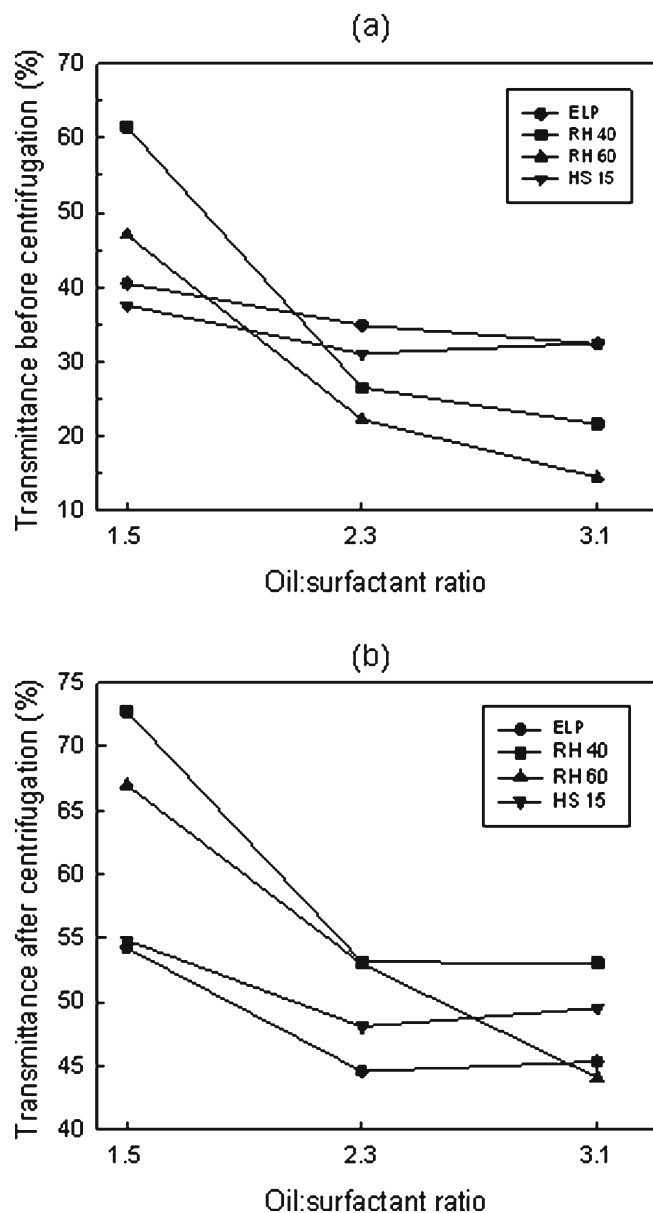[c] Bimodal distributions at 425 and 136 nm

Fig. 8. Interaction plots of the effects of surfactant type and oil/surfactant ratio on transmittance before centrifugation (**a**) and after centrifugation (**b**)

Reconstitution of Microemulsions from Self-emulsifying Pellets

In Fig. 7 typical plots of percentage transmittance (T%, before and after centrifugation) *vs* reconstitution time for Cremophor pellet batches with the mid oil/surfactant ratio 2.3 are presented. T%–time data for pellets with MCC alone is also shown for comparison. An abrupt decrease of T% (from 92.3% for deionized water) or increased turbidity is noticed within the first 2–15 min after immersion of the pellets in water, indicating rapid entrance of water and contact with the self-emulsifying mixture. After the first 20 min however, the rate of decrease of T% is slower.

From Fig. 7 it is noticed that transmittance is always higher after centrifugation (dash lines) than before (solid lines), which is explained due to the presence of disintegrated

MCC along with oil/surfactant droplets. In general, the difference in transmittance before and after centrifugation is small in the beginning but increases with reconstitution time. This implies that in the beginning turbidity arises mainly due to re-emulsification but after 15 min, where most of the pellets have completed disintegration (Table IV), it is very much influenced by the presence of disintegrated MCC. In addition, from Fig. 7 it can be seen that pellets with the more hydrophilic RH 60 (HLB=15.9) show lower transmittance or higher turbidity before centrifugation than ELP (HLB=13.9) and RH 40 (HLB=14.3). In general, the differences in transmittance between non-centrifuged samples are much larger than those between the centrifuged samples, implying that hydrophilicity mainly affects water penetration and disintegration and to a less extent the re-emulsification.

In Table VI the results of reconstitution testing after 180 min, for the 12 experimental batches of the factorial design and for the unpurified EL (at oil/surfactant ratio 2.3) are presented. In particular, the average diameter d and transmittance T% measured directly on the reconstitution medium representing dispersed mix of both disintegrated MCC and droplets, and the corresponding d_{cf} and T_{cf}%, measured after centrifugation, representing dispersed droplets alone, are given. From the data it appears that the average diameter is higher before than after centrifugation which is due to the presence of MCC of bigger size than the droplets. However, the differences are relatively small indicating disintegration of MCC in the form of fibrils, which agrees with the observation that pellets retained their spherical shape and did not break into smaller pieces during reconstitution. In addition, it is noticed that d_{cf} values are not very different to the corresponding diameters of the wetting microemulsions (dilution ×4, Table II).

From Table VI it is also noticed that increasing the oil/surfactant ratio, the values of both T% and T_{cf}% decrease. For the centrifuged samples for which turbidity arises purely from dispersed droplets, the decreased T% or increased turbidity and emulsion reconstitution can be ascribed to the lower surfactant content at high ratios of 2.3 and 3.1. This results in decreased gel formation prior to emulsification (Fig. 3, zone C) and therefore, shorter time to disrupt and penetrate the viscous gel and easier re-emulsification (25). For the non-centrifuged samples for which turbidity arises both from the dispersed droplets as well as MCC fibrils, the decreased T% at higher oil/surfactant ratios may be additionally ascribed to the easier movement of water inside the pellet due to the decreased gel, facilitating disintegration.

From Table VI, however, it is noticed that for formulations containing RH 60, all differences among the three ratios are high, whereas for the other surfactants only those between ratios 1.5 and 2.3 or 1.5 and 3.1, indicating interaction of the effects of the surfactant type and oil/surfactant ratio (Table V, $p=0.01$). This is demonstrated in the interaction plots in Fig. 8a and b where it can be seen further that for ratio 1.5, the transmittance before centrifugation is higher for the higher HLB grades of RH, compared to ELP with lower HLB, whereas at mid and high ratios this is reversed. Solutol appears less affected by the ratio. On the other hand, transmittance after centrifugation is generally higher for the RH grades than ELP and the difference is greater at ratio 1.5.

The lower transmittance after centrifugation or greater reconstitution of the microemulsions of ELP (Fig. 8b), may be

ascribed to its weaker H-bonding to MCC due to its lower hydrophilicity, and also, due to the double bond in the fatty acid (Fig. 1) which hinders molecular configuration and effective H-bonding with MCC as shown in the second derivative FT-IR spectra (Fig. 6b). This makes detachment and re-emulsification easier. The lower transmittance or higher turbidity before centrifugation of RH grades compared to ELP at mid and high ratio (Fig. 8a) can be ascribed to the increased disintegration. This is further supported by the total dispersed amount (oil/surfactant droplets and MCC fibrils) in the reconstitution medium after 180 min (calculated from the weight loss of pellets) given in Table VI. On average, the dispersed content increases with the HLB of the surfactant in the pellets, and except for ELP, it also increases with oil/surfactant ratio.

Comparing the data of purified ELP with the unpurified grade EL in Table VI, it can be seen that the value of T_{cf} for ELP is lower than that for EL, indicating greater emulsion reconstitution. This should be ascribed to the presence of free fatty acids and esters in EL, of lower emulsification ability than the main component (ester of glyceride with ethoxylated ricinoleic acid), as previously discussed for Fig. 2.

CONCLUSIONS

Hydrophilicity of Cremophors and Solutol in self-emulsifying mixtures incorporated in MCC pellets greatly affects the water requirements for their preparation, disintegration, and the reconstitution of microemulsions. Increasing oil/surfactant ratio increased the deformability of pellets. All surfactants form H-bonds with MCC in the order of increasing strength: ELP<RH 40<RH 60<HS 15. Incorporation of higher HLB surfactants resulted in faster and more extensive disintegration of the MCC fibrils. Pellet disintegration and microemulsion reconstitution increased with increasing oil/surfactant ratio due to decreased gel formation. The droplet size of reconstituted microemulsions was similar to that of the wetting microemulsion. It was also noticed that greater reconstitution was obtained from the purified ELP than the non-purified EL grade. Therefore, by appropriate selection of HLB and oil/surfactant ratio, highly spherical pellets with optimal disintegration providing good microemulsion reconstitution can be prepared for use in self-emulsifying drug delivery systems.

REFERENCES

1. Newton M, Petterson J, Podczeck F, Clarke A, Booth S. The influence of formulation variables on the properties of pellets containing a self-emulsifying mixture. J Pharm Sci. 2001;90:987–95.
2. Tuleu C, Newton M, Rose J, Euler D, Saklatvala R, Clarke A, Booth S. Comparative bioavailablity study in dogs of a self-emulsifying formulation of progesterone presented in a pellet and liquid form compared with an aqueous suspension of progesterone. J Pharm Sci. 2004;93:1495–502.
3. Newton JM, Godinho A, Clarke AP, Booth SW. Formulation variables on pellets containing self-emulsifying systems. Pharm Technol Europe. 2005;17:29–32.
4. Abdalla A, Mader K. Preparation and characterization of a self-emulsifying pellet formulation. Eur J Pharm Biopharm. 2007;66:220–6.
5. Podczeck F, Alessi P, Newton JM. The preparation of pellets containing non-ionic surfactants by extrusion/spheronization. Int J Pharm. 2008;361:33–40.
6. Podczeck F, Maghetti A, Newton JM. The influence of non-ionic surfactants on the rheological properties of drug/microcrystalline cellulose/water mixtures and their use in the preparation and drug release performance of pellets prepared by extrusion/spheronization. Eur J Pharm Sci. 2009;37:334–40.
7. Bachynsky MO, Shah NH, Patel CI, Malick AW. Factors affecting the efficiency of a self-emulsifying oral delivery system. Drug Dev Ind Pharm. 1997;23:809–16.
8. Pouton CW. Self-emulsifying drug delivery systems: assessment of the efficiency of emulsification. Int J Pharm. 1985;17:335–48.
9. Abdalla A, Klein S, Mader K. A new self-emulsifying drug delivery system (SEDDS) for poorly soluble drugs: characterization, dissolution, *in vitro* digestion and incorporation into solid pellets. Eur J Pharm Sci. 2008;35:457–64.
10. Florence AT, Attwood, D. Physicochemical principles of pharmacy. 2nd ed. The Macmillan Press, New York; 1988. p. 239–40.
11. Ditner C, Bravo R, Imanidis G, Kuentz MA. Systematic dilution study of self-microemulsifying drug delivery systems in artificial intestinal fluid using dynamic laser light scattering. Drug Dev Ind Pharm. 2009;35:199–208.
12. Podczeck F, Newton JM. A shape factor to characterize the quality of spheroids. J Pharm Pharmacol. 1994;46:82–5.
13. Balaxi M, Nikolakakis I, Kachrimanis K, Malamataris S. Combined effects of wetting, drying, and microcrystalline cellulose type on the mechanical strength and disintegration of pellets. J Pharm Sci. 2009;98:676–89.
14. Pouton CW. Formulation of self-emulsifying drug delivery systems. Adv Drug Deliv Rev. 1997;25:47–58.
15. Jeong SH, Park JH, Park K. In: Wassan KM, editor. Role of lipid-excipients in modifying oral and parenteral drug delivery. New Jersey: Wiley; 2007. p. 32–5.
16. Vervaet C, Baert L, Remon JP. Enhancement of *in vitro* drug release by using polyethylene glycol 400 and PEG-40 hydrogenated castor oil in pellets made by extrusion/spheronization. Int J Pharm. 1994;108:207–12.
17. Swenson ES, Milisen WB, Curatolo W. Intestinal permeability enhancement efficiency: acute local toxicity and reversibility. Pharm Res. 1994;11:1132–42.
18. Constantinides PP. Lipid microemulsions for improving drug dissolution and oral absorption: physical and biopharmaceutical aspects. Pharm Res. 1995;12:1561–72.
19. Pouton CW, Porter JHC. Formulation of lipid-based delivery systems for oral administration: materials, methods and strategies. Adv Drug Deliv Rev. 2008;60:625–37.
20. Shaw DJ. Introduction to colloid and surface chemistry. 3rd ed. London: Butterwoths; 1980. p. 85–6.
21. Strickley RG. Solubilizing excipients in oral and injectible formulations. Pharm Res. 2004;21:201–30.
22. Marechal Y, Chanzy H. The hydrogen bond network in Iβ cellulose as observed by infrared spectrometry. J Mol Struct. 2000;523:183–96.
23. Watanabe A, Morita S, Kokot S, Matsubara M, Fukai K, Ozaki Y. Drying process of microcrystalline cellulose studied by attenuated total reflection IR spectroscopy with two-dimensional correlation spectroscopy and principal component analysis. J Mol Struct. 2006;799:102–10.
24. Gardner KH, Blackwell J. The hydrogen bonding in native cellulose. Biochim Biophys Acta. 1974;343:232–7.
25. Nazzal S, Smalyukh II, Lavrentovich OD, Khan MA. Preparation and *in vitro* characterization of a eutectic based semisolid self-nanoemulsified drug delivery system (SNEDDS) of ubiquinone: mechanism and progress of emulsion formation. Int J Pharm. 2002;235:247–65.